Cellulose (2022) 29:6425–6440
https://doi.org/10.1007/s10570-022-04638-y

ORIGINAL RESEARCH

Durable superhydrophobic cotton fabric from cardanol/POSS-based polybenzoxazine for high-efficiency oil/water separation

Qianqian Shang · Jianwen Cheng · Caiying Bo · Yun Hu · Chengguo Liu · Xiaohui Yang · Lihong Hu · Yonghong Zhou · Wen Lei

Received: 26 October 2021 / Accepted: 8 May 2022 / Published online: 14 June 2022

Abstract Using biomass resources to develop high-performance superhydrophobic materials that can effectively separate oily wastewater has become an urgent demand. Herein, a novel biomass-based benzoxazine (C-aPOSS) from cardanol and aminopropyllsobutyl-POSS was designed and synthesized, and superhydrophobic cotton fabric (PC-aPOSS/CF) was constructed by dipping cotton fabric in C-aPOSS solution and then polymerizing in situ. The PC-aPOSS/CF exhibited high water contact angle of 155.0° ± 0.3° as well as excellent mechanical and chemical resistance. Due to its super-wettability and porosity, the superhydrophobic PC-aPOSS/CF possessed high separation performance for various oil/water mixtures with oil purities higher than 99.86% and oil fluxes above 3600 $L{\cdot}m^{-2}{\cdot}h^{-1}$. Furthermore, the superhydrophobic PC-aPOSS/CF and polyurethane sponge were used to prepare sandwich-like composite filter membrane for separating surfactant-free and surfactant-stabilized water-in-oil emulsions. The composite filter membrane exhibited oil purity greater than 99.93% and ultrahigh oil flux of over 127,289 L m^{-2} h^{-1} bar^{-1} in separating surfactant-free water-in-oil emulsions, and oil purity lager than 99.87% and oil flux higher than 17,895 L m^{-2} h^{-1} bar^{-1} in separating surfactant-stabilized water-in-oil emulsions. After operating 50 separation cycles of surfactant-free water-in-trichloromethane emulsion, oil purity was still above 99.99%, which indicates the outstanding recyclability of the composite filter membrane. Therefore, the development of high performance superhydrophobic PC-aPOSS/CF may provide a route to the oily wastewater treatment and oil purification.

Keywords Superhydrophobic · Cardanol · Cotton fabric · POSS · Oil/water separation

Supplementary Information The online version contains supplementary material available at https://doi.org/10.1007/s10570-022-04638-y.

Q. Shang · C. Bo · Y. Hu · C. Liu (✉) · X. Yang (✉) · L. Hu · Y. Zhou (✉)
Institute of Chemical Industry of Forest Products, CAF, Key Laboratory of Biomass Energy and Material, No 16, Suojin Wucun, Nanjing 210042, Jiangsu Province, China
e-mail: liuchengguo@icifp.cn

X. Yang
e-mail: yxh@icifp.cn

Y. Zhou
e-mail: zyh@icifp.cn

Q. Shang · C. Bo · Y. Hu · C. Liu · X. Yang · Y. Zhou
Co-Innovation Center of Efficient Processing and Utilization of Forest Resources, 159 Longpan Road, Nanjing 210037, Jiangsu Province, China

J. Cheng · W. Lei
College of Science, Nanjing Forestry University, 159 Longpan Road, Nanjing 210037, Jiangsu Province, China

Introduction

Oil bearing wastewater derived from oil spillage and industrial organic solvent discharge usually contains toxic substances, which have brought severe threats to aquatic ecosystems and even the health of human beings (Oliveira et al. 2021; Chen et al. 2019; Grabowski et al. 2017). Traditional technologies of isolating these pollutants usually suffer some limitations, such as high costs, and time consumption, resulting in secondary contamination, and low efficiency. Therefore, developing functional materials for high-efficiency separation of oil/water mixtures and emulsions has become an urgent demand.

Various functional materials, including meshes, sponges, aerogels, and fabrics, with superhydrophobicity/superoleophilicity (Shang et al. 2019, 2020; Zhang et al. 2020a, b; Renjith et al. 2021) have been designed and prepared for removing oils from wastewater owing to their high selectivity, high separation performance, and low energy consumption. Among these, cotton fabric has received broad attention because of its renewability, biodegradability, porosity, and good flexibility. Nevertheless, the intrinsic hydrophilicity of cotton fabric limits its application in oily wastewater treatment and oil purification. Hence, surface modification is highly demanded to transform cotton fabrics into superhydrophobic materials. A variety of approaches, such as dip-coating (Bai et al. 2020; Song et al. 2020), solvothermal reaction (Zhu et al. 2017; Ning et al. 2017), spray method (Park et al. 2020; Cao et al. 2020), electrophoretic deposition (Saji 2021; Ogihara et al. 2011), and chemical vapor deposition (Mosayebi et al. 2020; Zheng et al. 2009), have been developed for manufacturing superhydrophobic surfaces. All researches have proved that the combination of rough surface structure and low-surface-energy components is the most representative strategy in the design of superhydrophobic materials (Wang et al. 2020; Hu et al. 2020; Zhang et al. 2021; Si et al. 2018). Many studies have utilized nanoparticles to build micro/nano-roughness in superhydrophobic coatings (Shang et al. 2018; Bao et al. 2020). However, the roughness of the superhydrophobic surfaces based on nanoparticles is easily destroyed by mechanical abrasion, leading to the reduction of the superhydrophobicity. Furthermore, expensive fluorine-containing reagents are often utilized as low-surface-energy materials for superhydrophobic surfaces (Klimov et al. 2021; Zhang et al. 2018), which may increase costs and cause harm to human health and the environment. Therefore, the exploration of durable, nanoparticles-free, and fluorine-free superhydrophobic surfaces has become a research hotspot in the field oil–water separation.

As a new type of phenolic resin, benzoxazine is an important inexpensive alternative to prepare superhydrophobic surface because of its low cost, low water retention, mechanical robustness, and thermal stability (Wang et al. 2017; Malakooti et al. 2019; Zhang et al. 2020a, b; Qin et al. 2020). Benzoxazines with flexible molecular structure can be synthesized using phenols, primary amines, and formaldehyde through Mannich condensation reaction. Due to the shortage of petrochemical resources, the exploration of biomass with sustainable and renewable characteristics has received wide attention (Amarnath et al. 2019; Lyu and Ishida 2019). As a renewable phenol source, cardanol is a by-product of cashew nut shell processing. It has a C15 long aliphatic side chain with different degrees of unsaturation. Due to its renewability and commercially scalability, cardanol has been utilized as a substitute for petrochemical phenols to synthesize bio-based benzoxazine resin for oil–water separation (Prabunathan et al. 2020; Arumugam et al. 2021). For example, Arumugam et al. (2021) reported the oil–water separation efficiency of the cardanol-based polybenzoxazines coated cotton fabric was 95%. Yao et al. (2019) also reported the cardanol-based polybenzoxazine/SiO_2 modified fabric was used for separating of several heavy oils/water mixtures with oil fluxes in the range of 6500–9500 $L{\cdot}m^{-2}{\cdot}h^{-1}$ and separation efficiencies of all over 90%. Although excellent separation performance of cardanol-based superhydrophobic surfaces has been achieved for oil/water mixtures, the investigation for separating emulsified mixtures is still lacking. Recently, our group developed superhydrophobic cotton fabric with silylated cardanol-based polybenzoxazine for efficient separating of oil/water mixtures and emulsions through the sequential enzyme-etching, dip-coating, and thermal curing process (Shang et al. 2021). However, the enzyme-etching process for creating rough structure may limit the large-scale preparation of the superhydrophobic cotton fabric. Therefore, it is urgent to simplify the preparation process of cardanol benzoxazine-based superhydrophobic materials for oil/water emulsion separation.

In this work, a novel cardanol/POSS-based benzoxazine (C-aPOSS) was synthesized by using cardanol, paraformaldehyde and aminopropyllsobutyl-POSS through Mannich condensation. Then, a durable superhydrophobic cardanol/POSS-based polybenzoxazine (PC-aPOSS) coated cotton fabric was fabricated through dip-coating technique and thermal curing process. Thanks to the rigid cubic cage structure of POSS, a hierarchical rough structure was formed on the surface of the modified cotton fabric without additional treatment. Excellent mechanical and chemical durability of the modified cotton fabric were observed because of the remarkable chemical and physical stability of the PC-aPOSS. Due to its superhydrophobic and superoleophilic properties, the modified cotton fabric exhibited high performance in the separation of a variety of oil/water mixtures and emulsions. This simple and facile synthesis approach provides an avenue for large-area creation of superhydrophobic materials for oily wastewater treatment.

Experimental section

Materials

Cardanol was supplied by Jining Huakai Resin Co., Ltd. Aminopropyllsobutyl-POSS (NH_2-POSS) was purchased from Hybrid Plastics (USA). Oil red, Span80, cyclohexane, paraformaldehyde and petroleum ether were obtained from Energy Chemical (Shanghai). Absolute ethanol, toluene, 1, 4-dioxane, trichloromethane, dichloromethane and dichloroethane were purchased from Nanjing Chemical Reagent Co., Ltd. Cotton fabric (Material: 100% cotton; Style: plain woven; Fabric Squared Weight: 150 $g{\cdot}m^{-2}$; Yarn Count: 20S*20S; Ends Picks: 60*60) was purchased from local mall.

Synthesis of C-aPOSS

Paraformaldehyde (0.4 mol), cardanol (0.2 mol) and NH_2-POSS (0.2 mol) were added into a round-bottom flask and then dissolved in 200 mL of 1, 4-dioxane. The solution was heated to 90 °C and refluxed for 8 h. After the reaction, reddish-brown C-aPOSS was obtained by removing the solvent using rotary evaporation.

Fabrication of PC-aPOSS/CF

CF was washed using an ethanol/water mixture to remove the surface impurities before use. C-aPOSS was dissolved in absolute ethanol at concentrations of 1.0 wt.%, 1.5 wt.%, 2.0 wt.%, 2.5 wt.% and 3.0 wt.%. Subsequently, CF (3 cm × 3 cm) was immersed in 50 mL of different C-aPOSS concentration ethanol solution for 30 min, then taken out and dried at 70 °C for 30 min. After further heating at 190 °C for 1 h, the polybenzoxazine coated CF (PC-aPOSS/CF) was formed. In addition, PC-aPOSS/CF was prepared by immersing CF in the 2.0 wt% C-aPOSS solution with different time (10 ~ 60 min) to study the effect of dipping time on the hydrophobicity.

Characterizations

The surface morphologies and elements of the samples were analyzed by Field Emission Scanning Electron Microscopy (FE-SEM, Zeiss supra 55) equipped with an Energy Dispersive Spectrometer (EDS). The 3D topography and surface roughness of the samples were detected by using a Confocal Laser Scanning Microscopy (CLSM, KEYENCE VK-150 K). The chemical structure of the samples was analyzed by Fourier Transform infrared spectroscopy (FT-IR, Nicolet iS 10) and X-ray photoelectron spectroscopy (XPS, ESCALAB250Xi). The water contact angle (WCA) and sliding angle (SA) of the samples were recorded by a contact angle meter (CV-705B, CVOK, Dongguan) with 5 μL of water. At least five positions were measured for each sample. The emulsion droplet images were characterized using an Olympus Optical Microscope (BH53). The size distributions of the emulsion droplets were tested using a Mastersizer 2000. The air permeability of the samples was characterized by using a fabric permeability instrument (YG461E) with an operating pressure of 100 Pa. The test of mechanical property was performed on a UTM 4304 universal tester with a speed of 2 $mm{\cdot}min^{-1}$.

Mechanical durability and environmental stability

The mechanical durability of the PC-aPOSS/CF was investigated by abrasion test and ultrasound treatment. In the abrasion test, the PC-aPOSS/CF (3.0 cm × 3.0 cm) placed on 1000 grit sandpaper, loaded with a weight of 200 g, and then moved

linearly by 10 cm for an abrasion cycle. The WCA and SA were recorded every 10 cycles. In the ultrasound treatment, the PC-aPOSS/CF was dipped into ultrapure water and put into the ultrasonic cleaning machine (KH7200DB, Hechuang Ultrasonic). The WCA and SA were evaluated every 10 min.

The corrosive resistance was tested to evaluate the durability of the PC-aPOSS/CF in harsh operating environment. For the corrosive resistance, corrosive liquids with pH value between 1 and 13 were prepared by diluting HCl and NaOH solutions. The corrosive liquids were dropped on the PC-aPOSS/CF surface and then the WCA was recorded. Furthermore, PC-aPOSS/CF was immersed in HCl solution (1 M) or NaOH solution (1 M) for 24 h to investigate its corrosive resistance.

Oil/water separation

Toluene, cyclohexane, petroleum ether, trichloromethane, dichloromethane and dichloroethane were chosen for oil/water separation experiment. Oil/water mixtures were prepared by mixing oils with ultrapure water in a volume ratio of 1:1. Surfactant-free water-in-oil emulsions were prepared by mixing ultrapure water and oils (v: v, 1:99) using an emulsion machine (T10, IKA) at 10,000 rpm for 10 min. Six kind of surfactant-stabilized water-in-oil emulsions were prepared by adding Span80 (1 g) and ultrapure water (10 ml) into oils (90 ml) respectively. The mixtures were emulsified at 10,000 rpm for 10 min to obtain the stable emulsions.

The experiment for separating oil/water mixtures was performed on the homemade separation device by gravity using a piece of PC-aPOSS/CF as the filter membrane. For separating surfactant-free and surfactant-stabilized water-in-oil emulsions, a polyurethane (PU) sponge was wrapped by two pieces of PC-aPOSS/CF to form sandwich-like composite filter membrane. The separation experiment was performed under external pressure (0.2 bar). The water content in the filtrate was tested by using a Karl Fischer Moisture Titrator (Mettler Toledo, ET-08). The oil purity was calculated according to the water content in the filtrate.

The fluxes for oil/water mixture and emulsion were measured according to Eqs. (1) and (2) respectively.

$$\text{Flux} = \frac{V}{A \times t} \quad \left(\text{L m}^{-2}\ \text{h}^{-1}\right) \tag{1}$$

$$\text{Flux} = \frac{V}{A \times t \times P} \quad \left(\text{L m}^{-2}\ \text{h}^{-1}\ \text{bar}^{-1}\right) \tag{2}$$

where V is the oil volume (L), A is the separation area (m^2), t is the separation time (h) and P is the operating pressure (bar).

The repeated flux and oil purity for the oil/water mixture and emulsion were recorded to evaluate the reusability of the PC-aPOSS/CF. The contaminated PC-aPOSS/CF was cleaned by using ethanol and dried after each cycle for further use.

Results and discussion

Synthesis and characterization of C-aPOSS

A novel C-aPOSS monomer was synthesized through Mannich condensation reaction between cardanol, paraformaldehyde and NH_2-POSS. The synthesis route of C-aPOSS is revealed in Fig. 1a. The chemical structure of C-aPOSS was characterized by FT-IR and ^{1}H NMR. Figure 1b displays the FT-IR spectra of cardanol, NH_2-POSS and C-aPOSS. In the C-aPOSS spectrum, the typical peak at 1253 cm^{-1} for the C–O–C asymmetric vibration, the peak at 1365 cm^{-1} for the C–N–C bending vibration and the peak at 887 cm^{-1} for the oxazine ring attached in the benzene ring were detected (Devaraju et al. 2019), which indicated the successful formation of the benzoxazine structure. The peaks at 2953, 2924 and 2853 cm^{-1} were assigned to the stretching vibrations of methyl and methylene groups on the long alkyl carbon chain of cardanol and the isobutyl of NH_2-POSS. The peak at 1462 cm^{-1} confirmed the C–H asymmetrical deformation vibration, whereas the peaks at 3008 and 1587 cm^{-1} revealed the unsaturated double bond and the benzene ring structure of cardanol. Also, the peak at 1094 cm^{-1} denoted the asymmetric stretching vibration of Si–O–Si group. Figure 1c reveals the ^{1}H NMR spectrum of C-aPOSS. From the spectrum, the peaks of oxazine ring were appeared at 3.75–3.95 (a) and 4.70–4.90 (b) ppm, which were ascribed to Ar–CH_2–N– and –O–CH_2–N– groups respectively. The peaks detected at 2.27 (c) and 1.58 (d) ppm correlated with the propyl chain of –N–CH_2–C– and

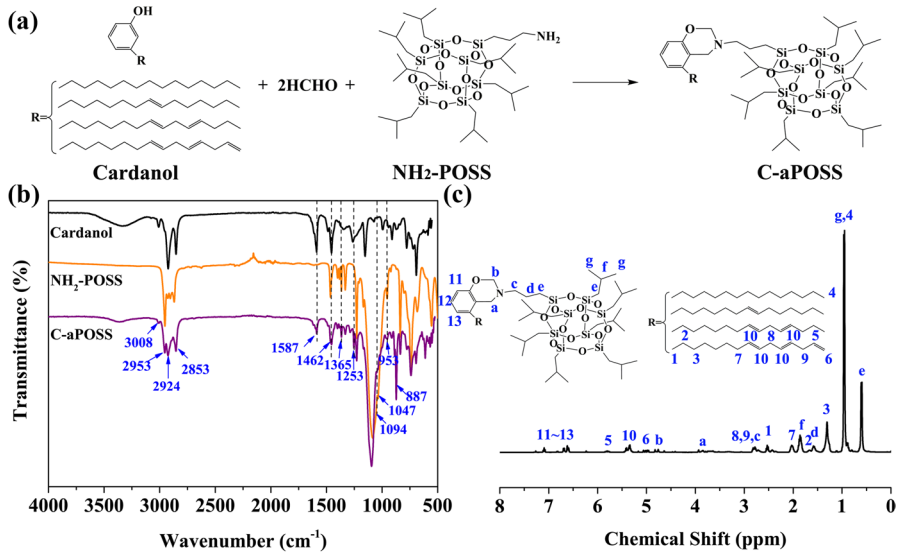

Fig. 1 **a** Synthesis route of C-aPOSS. **b** FT-IR spectra of cardanol, NH_2-POSS and C-aPOSS. **c** ^{1}H NMR spectrum of C-aPOSS

–C–CH_2–C groups respectively. The methylene peak of –C–CH_2–Si– group was detected at 0.57–0.62 (e) ppm. The methylene peak of NH_2-POSS was observed at 1.85 (f) ppm. The peaks for the methyl protons of cardanol and NH_2-POSS appeared at 0.85–0.91 (4) and 0.92–1.00 (g) ppm respectively. The peaks at 5.00 (6), 5.35 (5) and 5.80 (10) ppm corresponded to the unsaturated protons of cardanol. The peaks at 6.48–7.15 (11 ~ 13) ppm were assigned to the aromatic groups of cardanol. The peaks at 1.34 (3), 1.65 (2), 2.05 (8, 9) and 2.85 (7) ppm were attributed to the methylene protons of the long alkyl chain of cardanol. These results demonstrate that the C-aPOSS was successfully synthesized from cardanol and NH_2-POSS.

Fabrication of superhydrophobic PC-aPOSS/CF

The schematic preparation strategy of superhydrophobic PC-aPOSS/CF is presented in Fig. 2. Initially, C-aPOSS was dispersed in ethanol to prepare a uniform dispersion. The C-aPOSS coated CF (C-aPOSS/CF) was prepared by immersing a piece of pristine CF into the C-aPOSS ethanol solution with ultrasonic treatment for 30 min. After drying at 70 °C for 30 min, the C-aPOSS/CF was cured at 190 °C for 1 h

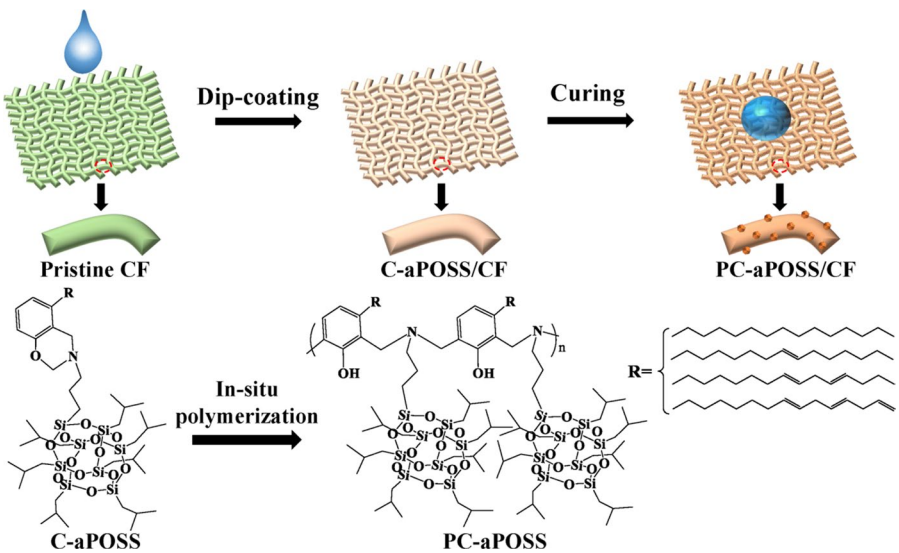

Fig. 2 Schematic diagram of fabrication of superhydrophobic PC-aPOSS/CF by in-situ polymerization

to obtain the superhydrophobic PC-aPOSS/CF. The C-aPOSS monomers was polymerized on the fiber surface through thermal treatment ring-opening reaction to form polybenzoxazine. During the polymerization process, the C–O bond of the oxazine ring was cleaved and reacted with the aromatic ring of another C-aPOSS molecule, which resulted in a cross-linking network structure of polybenzoxazine on the fiber.

It is well known that low-surface-energy chemistry and hierarchical rough structure are essential for the fabrication of superhydrophobic surfaces. Herein, the polybenzoxazine PC-aPOSS was used as the low-surface-energy material due to the oxazine rings and long alkyl chains in its molecule, while the hierarchical rough morphology on the CF surface originated from the agglomeration of the PC-aPOSS polymers.

The effect of C-aPOSS concentration on the surface morphology and hydrophobicity of the PC-aPOSS/CF was investigated, as shown in Fig. 3a–g. The changes of 3D topography and roughness of the PC-aPOSS/CF with different C-aPOSS concentrations were characterized by CLSM (Figure S1). Figure 3a shows that the fiber of the pristine CF had a flat surface with intrinsic winkles. The surface profile of the pristine CF showed the interweaving structure of fibers with an arithmetic average of the roughness profile (Sa) of 24.2 μm (Figure S1(a)). The pristine CF had a WCA of 0° and an oil contact angle of 0° (Fig. 5a), indicating its intrinsic superhydrophilicity/superoleophilicity. After coating PC-POSS, the surface profiles of the PC-aPOSS/CF were similar with that of the pristine CF, but the values of Sa changed significantly (Figure S1(b-f)). When the concentration of C-aPOSS was 1.0 wt.%, the intrinsic winkles of the fiber were filled by the PC-aPOSS polymers and the rough structure was formed on the fiber surface due to the agglomeration of POSS in the polybenzoxazine (Fig. 3b). The Sa of the PC-aPOSS/CF for 1.0 wt.% C-aPOSS increased to 25.4 μm (Figure S1(b)). The PC-aPOSS/CF for 1.0 wt.% C-aPOSS had a WCA of 149.5° ± 1.2° and a SA of 7.2° ± 0.6° (Fig. 3g), indicating its high hydrophobicity. Increasing the C-aPOSS concentration to 1.5 wt.%, more POSS aggregates were formed on the fiber surface with increasing roughness (Sa = 27.1 μm), as shown in Fig. 3c and Figure S1(c). The WCA of PC-aPOSS/CF for 1.5 wt.% C-aPOSS increased to 152.2° ± 1.1° (Fig. 3g), demonstrating the superhydrophobicity of the PC-aPOSS/CF. When the C-aPOSS concentration was 2.0 wt.% (Fig. 3d), the fiber surface was

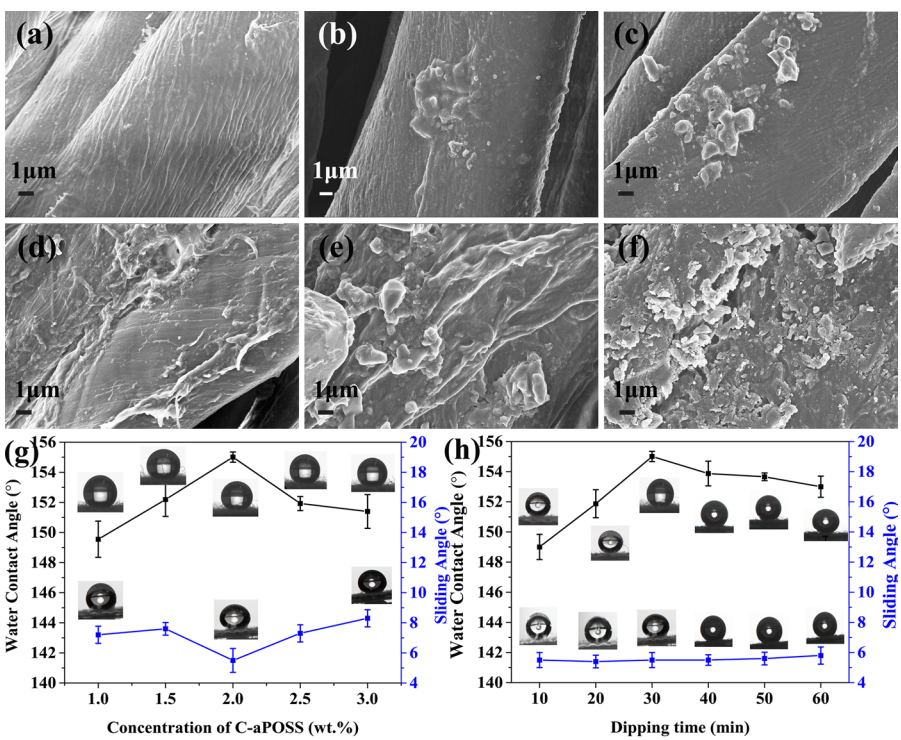

Fig. 3 SEM images of the CF (**a**) and PC-aPOSS/CF prepared with different C-aPOSS concentrations (1.0 wt.% (**b**), 1.5 wt.% (**c**), 2.0 wt.% (**d**), 2.5 wt.% (**e**) and 3.0 wt.% (**f**)). Effects of (**g**) C-aPOSS concentration and (**h**) dipping time on WCA and SA of the PC-aPOSS/CF

covered by many protuberances with a roughness of Sa = 31.2 μm (Figure S1(d)). The PC-aPOSS/CF had a maximum WCA of 155.0° ± 0.3° and a minimum SA of 5.5° ± 0.5° (Fig. 3g). These results indicated that the superhydrophobic surface of the PC-aPOSS/CF was in the Cassie-Baxter state. According to the Cassie-Baxter theory (Cassie and Baxter, 1944), the pores and intervals between the fibers and rough structures could trap masses of air to provide a composite surface. The trapped air formed a cushion layer, which could effectively prevent water droplets from penetrating into the composite surface interior, resulting in superhydrophobicity. With the further increasing of C-aPOSS concentration to 2.5 wt.% and 3.0 wt.%, the continuous polymer coatings with massive POSS aggregates were formed on the fiber surfaces (Fig. 3e, f). However, the roughness of the PC-aPOSS/CF was reduced to Sa = 29.6 μm for 2.5 wt.% C-aPOSS (Figure S1(e)) and Sa = 29.2 μm for 3.0 wt.% C-aPOSS (Figure S1(f)), which might be caused by filling excess PC-aPOSS in the gaps between the fibers. Accordingly, the WCA of the PC-aPOSS/CF decreased to 151.9° ± 0.5° for 2.5 wt.% C-aPOSS and 151.4° ± 1.1° for 3.0 wt.% C-aPOSS (Fig. 3g). Thus, the 2.0 wt.% C-aPOSS solution was used in the follow-up study.

Furthermore, the effect of dipping time on the hydrophobicity and surface morphology of the PC-aPOSS/CF with 2.0 wt.% C-aPOSS was studied (Fig. 3h and Figure S2). The dipping time of the CF in C-aPOSS solution could also affect the loading content of PC-aPOSS on the CF (Figure S2). Figure 3h shows that the WCA and SA of the PC-aPOSS/CF altered with dipping time and the most appropriate one was 30 min. Further increasing the dipping time could cause an aggregation of PC-aPOSS and decrease the surface roughness (Figure S2), which resulted in the reduction of the hydrophobicity. Therefore, the superhydrophobic PC-aPOSS/CF prepared with 2.0 wt.% C-aPOSS and 30 min dipping time was chosen for the following studies.

Chemical structure and composition of the PC-aPOSS/CF

The chemical structure of the C-aPOSS, pristine CF and PC-aPOSS/CF were characterized by FT-IR (Fig. 4a). In the spectrum of PC-aPOSS/

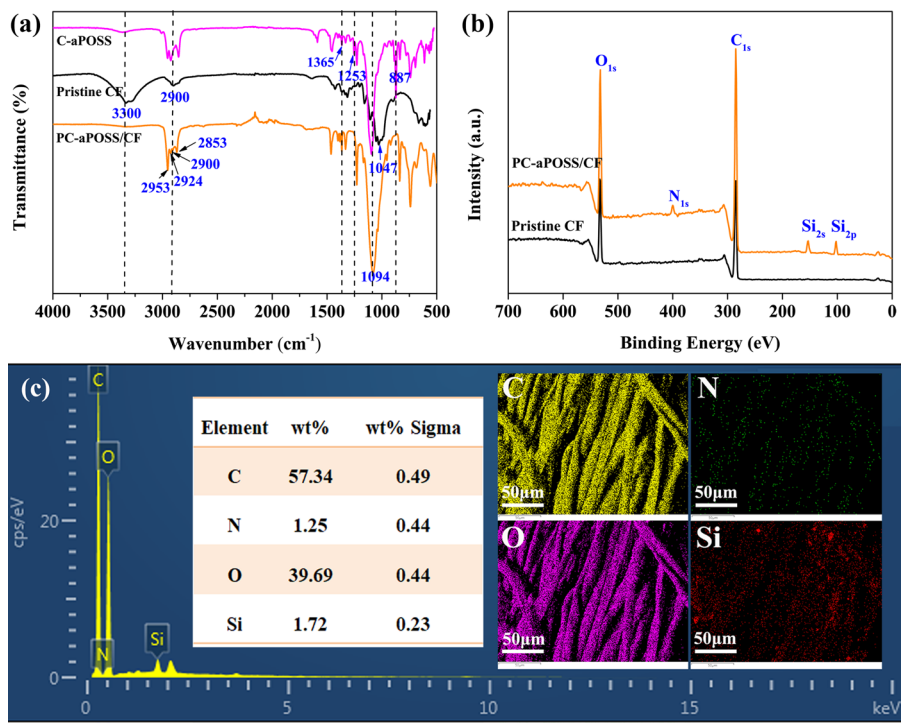

Fig. 4 **a** FT-IR spectra of the C-aPOSS, pristine CF and PC-aPOSS/CF. **b** XPS spectra of the pristine CF and PC-aPOSS/CF. **c** EDS spectrum and element mappings of PC-aPOSS/CF

CF, the peaks of the oxazine ring at 1365, 1253 and 887 cm^{-1} disappeared, indicating that the C-aPOSS monomer was completely cross-linked and polymerized to form polybenzoxazine. Meanwhile, some new peaks were detected in the spectrum of PC-aPOSS/CF compared with that the pristine CF. The peaks at 2953, 2924 and 2853 cm^{-1} were assigned to the methyl and methylene stretching vibrations of the long alkyl carbon chain of cardanol moiety and the isobutyl groups of NH_2-POSS. And the Si–O–Si peak was detected at around 1094 cm^{-1} in the PC-aPOSS/CF. XPS was used to further characterize the chemical compositions of the pristine CF and PC-aPOSS/CF. As revealed in Fig. 4b, the surface of the pristine CF was mainly composed of C and O elements. However, C, N, O and Si elements were detected on the surface of the PC-aPOSS/CF. The N element showed a peak at 399.9 eV (N 1 s), and the Si element displayed two peaks at 102.3 eV (Si 2p) and 153.1 eV (Si 2 s), indicating the presence of PC-aPOSS on the surface of the cotton fabric. EDS results further proved that the C, O, N and Si elements were the main components of the superhydrophobic PC-aPOSS/CF, as shown in Fig. 4c. The element mappings in Fig. 4c reveal that the PC-aPOSS coating successfully covered the surface of cotton fabric.

Superhydrophobicity/superoleophilicity of PC-aPOSS/CF

The super-wettability of pristine CF and PC-aPOSS/CF were investigated. As shown in Fig. 5a, the water-based liquids and cyclohexane could spread on the surface of the pristine CF, which confirmed the superhydrophilicity/superoleophilicity of the pristine CF. Figure 5b shows that the water-based liquids even including corrosive liquids were repelled by the PC-aPOSS/CF and formed ball-like shapes due to the superhydrophobicity of the PC-aPOSS/CF. However, cyclohexane was adsorbed upon contact with PC-aPOSS/CF, indicating the superoleophilicity of the PC-aPOSS/CF. The superoleophilicity was attributed to the oleophilicity of the alkyl chains in the PC-aPOSS, which was enhanced by the rough structure of the PC-aPOSS/CF. In addition, after modifying PC-aPOSS coating, the color of the cotton fabric changed from white to yellowish-brown (Fig. 5a, b), which was caused by the reddish-brown color of cardanol-based benzoxazine monomer and the yellowing of the benzoxazine monomer after polymerization (Li et al. 2018). However, the PC-aPOSS/CF exhibited uneven color due to the aggregation of the benzoxazine monomers caused by the rapid evaporation of ethanol during drying.

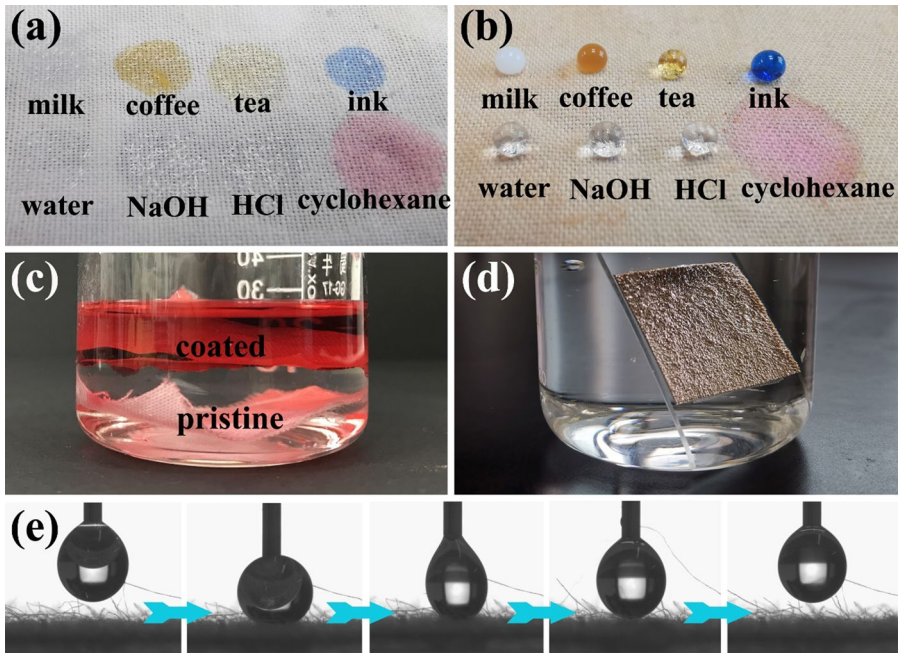

Fig. 5 Photographs of water-based droplets and cyclohexane on (**a**) pristine CF and (**b**) PC-aPOSS/CF. **c** PC-aPOSS/CF on the oil–water interface. **d** Mirror-like phenomenon of PC-aPOSS/CF underwater. **e** Low adhesion between PC-aPOSS/CF and water droplet

Figure 5c exhibits that the pristine CF sank to the bottom due to its superhydrophilicity, while PC-aPOSS/CF could float on the interface of oil and water phases because of its superhydrophobicity/superoleophilicity. Figure 5d shows that the PC-aPOSS/CF exhibited a mirror-like phenomenon after immersing in water because of the trapped air in the rough surface, confirming its excellent superhydrophobicity. As shown in Fig. 5e, the low adhesion of the PC-aPOSS/CF to water droplet was investigated. After the process of approaching, deforming and leaving, the water droplet could be completely separated from the PC-aPOSS/CF surface, which demonstrated the ultralow adhesion between the PC-aPOSS/CF and water droplet.

Mechanical durability and environmental stability of PC-aPOSS/CF

In real-world applications, superhydrophobic surfaces usually lose their superhydrophobicity due to the damage of rough structure and depletion of low-surface-energy component after exposure to abrasion, ultrasound, or acid/alkali environment. In this work, the abrasion test and ultrasound treatment were used to investigate the durability of the PC-aPOSS/CF. Figure 6a exhibits the change of WCA and SA with abrasion cycles. The PC-aPOSS/CF had a WCA of 147.0° ± 0.5° and a SA of 14.5° ± 1.0° even after 200 sandpaper abrasion tests, indicating its great mechanical durability. In addition, Fig. 6b displays the wettability of the PC-aPOSS/CF after ultrasonic shaking in water for different time. After ultrasonic shaking for 60 min, the WCA was maintained at 147.7° ± 0.6° and the SA was lower than 9°, demonstrating that the PC-aPOSS/CF had outstanding ultrasonic resistance. The excellent mechanical durability of the superhydrophobic PC-aPOSS/CF prepared by this method might be due to the intrinsic stability of POSS and the cross-linking structure of polybenzoxazine.

To explore the stability of the PC-aPOSS/CF under aqueous acid and alkaline solutions, the WCA and SA of corrosive liquids (pH = 1 ~ 13) on the PC-aPOSS/CF surface were measured (Fig. 6c). Compared with pure water, the CAs of corrosive liquids was reduced because the corrosive liquids destroyed the Si–O–Si bonds of POSS in the polybenzoxazine coating. However, the PC-aPOSS/CF could maintain high hydrophobicity after soaking in acid and alkaline solutions for 24 h (Fig. 6d), demonstrating that it had great chemical corrosion resistance.

Subsequently, the mechanical properties and air permeability of the pristine CF and PC-aPOSS/CF were investigated, as shown in Table 1. It can be seen from the table, the tensile strength and elongation at break of the PC-aPOSS/CF decreased compared with that of the pristine CF, which was caused by the high temperature treatment during the thermal curing

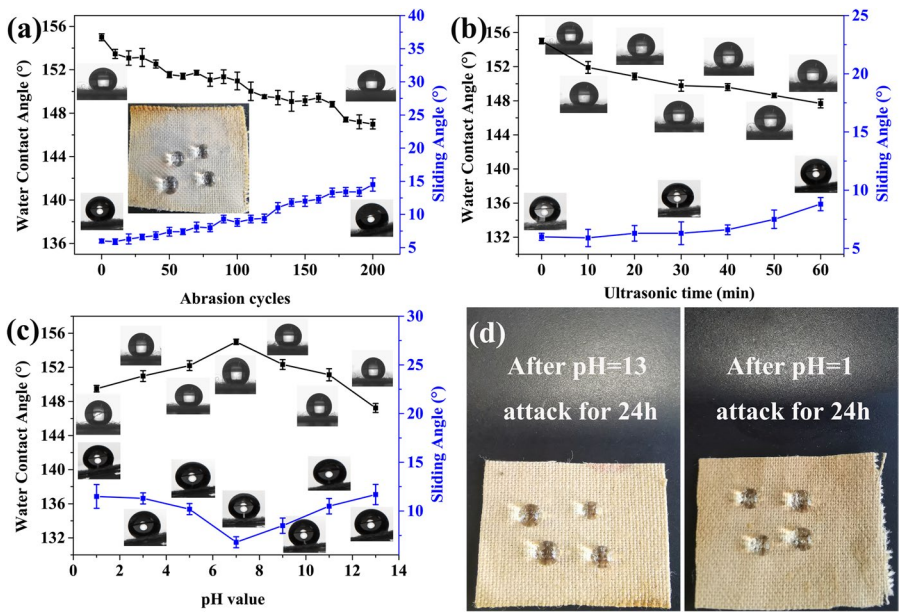

Fig. 6 The changes of the WCA and SA of the PC-aPOSS/CF with (**a**) different abrasion cycles and (**b**) different ultrasonic time. **c** WCA and SA of corrosive liquids (pH = 1 ~ 13) on the PC-aPOSS/CF. **d** Photographs of the PC-aPOSS/CF after soaking in acid and alkaline solutions for 24 h

Table 1 Physical properties of the pristine CF and PC-aPOSS/CF

Property	Pristine CF	PC-aPOSS/CF
Tensile strength (MPa)	28.3 ± 2.2 (warp)	27.5 ± 5.1 (warp)
	18.6 ± 4.7 (weft)	18.4 ± 2.6 (weft)
Elongation at break (%)	12.4 ± 2.9 (warp)	8.3 ± 1.5 (warp)
	19.4 ± 4.3 (weft)	16.4 ± 2.3 (weft)
Air permeability ($mm{\cdot}s^{-1}$)	355 ± 21	207 ± 17

process. In addition, the air permeability of the fabric was also reduced after the modification of PC-aPOSS coating, which might be due to the reduction of the gaps between the fibers by the loaded polybenzoxazine resin.

Separation of oil/water mixtures

Taking the advantages of the superhydrophobility/superoleophilicity, the as-prepared PC-aPOSS/CF is very suitable for oil/water separation. As revealed in Fig. 7a, b, a homemade filter equipment with the PC-aPOSS/CF as filter element was used to separate various oil/water mixtures. A variety of light oils and weight oils were employed as models for the oil/water separation. The fluxes of pure oils were measured (Fig. 7c). The fluxes of toluene, petroleum ether, cyclohexane, dichloromethane, trichloromethane and dichloroethane were 5587 ± 34, 5954 ± 45, 4075 ± 26, 10,431 ± 416, 8810 ± 437 and 6050 ± 25 $L{\cdot}m^{-2}{\cdot}h^{-1}$ respectively. The flux difference was mostly related to the densities of the used oils/organic solvents. Due to the impediment of water, the fluxes of the light oil/water mixtures were dramatically lower than that of the pure oils, but they were still higher than 3600 $L{\cdot}m^{-2}{\cdot}h^{-1}$ (Fig. 7d). The oil purities towards these oil/water mixtures were all higher than 99.86% (Fig. 7d). Particularly, the oil purities of petroleum ether and cyclohexane reached 99.99%, which was greater than other superhydrophobic fabrics (Pal et al. 2021; Yao et al. 2020; Lu et al. 2020; Xu et al. 2020; Sam et al. 2021). Furthermore, the recyclability of the PC-aPOSS/CF for separating trichloromethane/water mixture was investigated, as shown in Figure S3. After 50 separation cycles, the oil purity of trichloromethane was higher than 99.90% and the oil flux was remained at 8000 $L{\cdot}m^{-2}{\cdot}h^{-1}$, demonstrating the long-term recyclability of the PC-aPOSS/CF. Figure S4 shows the WCA and SA of the PC-aPOSS/CF after different separation cycles. The WCA decreased and the SA slightly increased with the increase of separation cycles. However, after 50 separation cycles, the WCA remained above 150° and the SA was lower than 7°, which indicated the robust superhydrophobicity of the PC-aPOSS/CF.

Separation of water-in-oil emulsion

In addition to the immiscible oil/water mixture, water-in-oil emulsions also have adverse effects on oil quality because of their stability and small size. Here, a composite filter membrane with sandwich structure was designed by wrapping a polyurethane (PU) sponge with two pieces of PC-aPOSS/CF (PC-aPOSS/CF@PU sponge@ PC-aPOSS/CF) (Fig. 8a). Due to the large interspace between interwoven fibers of the cotton fabric, low oil purity (~ 85%) was obtained by directly using PC-aPOSS/CF as a filter membrane. Consequently, the designed composite filter membrane was employed to improve the oil purity. Six kinds of surfactant-free water-in-oil emulsions, including water-in-toluene, water-in-petroleum ether, water-in-cyclohexane, water-in-dichloromethane, water-in-trichloromethane and water-in-dichloroethane, were prepared as working solutions for separation experiments. As depicted in Fig. 8b, the oil fluxes for the tested surfactant-free emulsions were 170,089 ± 8021, 245,930 ± 6403, 158,731 ± 4705, 248,954 ± 10,437, 166,627 ± 3874 and 127,289 ± 9977 $L{\cdot}m^{-2}{\cdot}h^{-1}{\cdot}bar^{-1}$. The oil purities of these surfactant-free emulsions were all higher than 99.93% (Fig. 8b). The water-in-cyclohexane emulsion was milky white liquid and numerous water droplets were detected in the optical microscope image (Fig. 8c). After filtering, the filtrate became clear and transparent, and almost no water droplets were observed in the filtrate (Fig. 8c). The other five emulsions presented similar results after separation with the designed composite filter membrane (Figure S5). Figure 8d, e reveals that the size distribution of water droplets in emulsion and filtrate. After filtration with the PC-aPOSS/CF@PU sponge@PC-aPOSS/CF composite filter membrane, the size distribution of water droplets in the filtrate was 0.6 ~ 1.5 nm, demonstrating its outstanding separation performance.

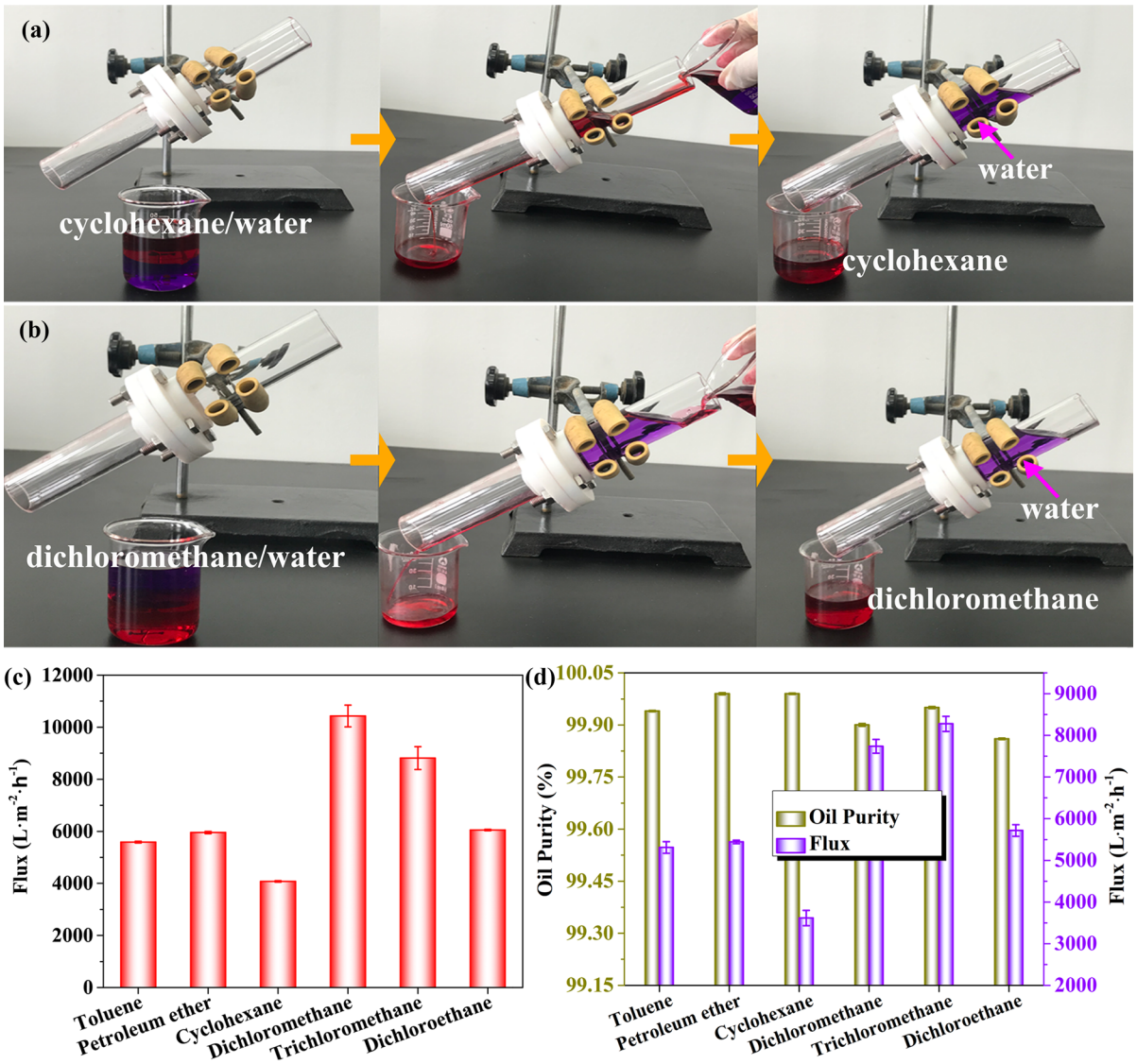

Fig. 7 The process of oil/water separation: **a** cyclohexane/water mixture, **b** dichloromethane/water mixture. **c** Fluxes of various pure oils. **d** Oil purities and fluxes of various oil/water mixtures

It is noteworthy that the improved oil purity of the PC-aPOSS/CF@PU sponge@PC-aPOSS/CF composite filter membrane compared with that of the single PC-aPOSS/CF was due to the great adsorption ability of the PU sponge for the tiny water drops passing through the top layer of PC-aPOSS/CF. The comparison of the separation performance with the previously reported superhydrophobic separation materials is shown in Table 2. Compared with other separation materials, the composite filter membrane exhibited comparable or higher separation performance and flux for the tested water-in-oil emulsions. The recyclability of the composite filter membrane was assessed by using the cyclic separation tests of surfactant-free water-in-trichloromethane emulsion, as illustrated in Figure S6. The oil purity of the composite filter membrane was remained above 99.99% even after 50 separation cycles. The flux presented a slight decrease at the initial 5 separation cycles and had no significant fluctuation in the following separation process. After 50 separation cycles, the flux was maintained at 128,691 $L{\cdot}m^{-2}{\cdot}h^{-1}{\cdot}bar^{-1}$. These

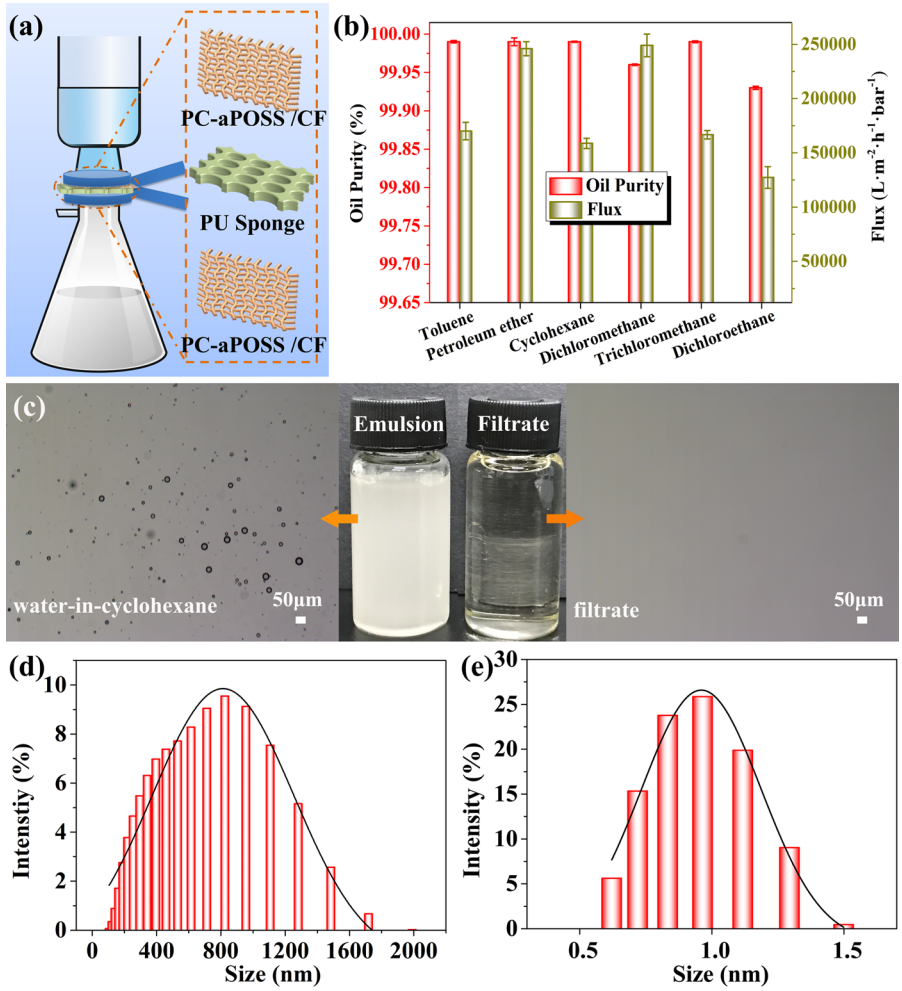

Fig. 8 **a** Separation setup for water-in-oil emulsion. **b** Oil purities and fluxes for six kinds of surfactant-free water-in-oil emulsions. **c** Photograph and optical microscope images of the surfactant-free water-in-cyclohexane emulsion before and after the filtration. Size distributions of surfactant-free water-in-cyclohexane emulsion (**d**) and filtrate (**e**)

results proved that the composite membrane had the outstanding separation performance and long-term durability.

To further study the separation ability of the composite filter membrane, six kinds of surfactant-stabilized water-in-oil emulsions with water volume fraction of 10% were prepared. As shown in Fig. 9, the oil purities of all the surfactant-stabilized emulsions were higher than 99.87%, with a few up to 99.99%, indicating the excellent separation efficiencies. The fluxes of the six surfactant-stabilized water-in-oil emulsions based on an external pressure were 26,786 ± 1120, 30,157 ± 2170, 27,087 ± 1274, 25,956 ± 1805, 19,390 ± 3251 and 17,895 ± 2527 L m^{-2} h^{-1} bar^{-1} for toluene, petroleum ether, cyclohexane, dichloromethane, trichloromethane and dichloroethane respectively (Fig. 9). The oil purities of the surfactant-stabilized emulsions were close to those of surfactant-free emulsions. Although the fluxes were lower than those of the surfactant-free emulsions, they were still extremely high compared to those of other separation materials, such as a ZnO nanoflower@SiC composite ceramic membrane with a flux of ~ 1300 L m^{-2} h^{-1} bar^{-1} (Wei et al. 2022) and MnO_2 & Carbon sphere composite membrane with fluxes in the range of 3032–15,199 L m^{-2} h^{-1} bar^{-1} (Chen et al. 2022). To clearly observe the effectiveness of this separation process, the optical microscope images of both emulsion and filtrate using surfactant-stabilized water-in-toluene emulsion as an example are shown in Figure S7. The emulsion was obviously converted into transparent liquid after being filtered. No droplets were observed in the filtrate, indicating the outstanding performance of the composite filter

Table 2 Comparison of the separation properties of various superhydrophobic materials for separating of water-in-oil emulsions

Superhydrophobic materials	Emulsion type	Oil purity (%)	Flux ($L{\cdot}m^{-2}{\cdot}h^{-1}$) (Gravity-driven)	Flux ($L{\cdot}m^{-2}{\cdot}h^{-1}{\cdot}bar^{-1}$) (Pressure-driven)	References
SWCNT-based bilayer membrane	surfactant-stabilized water-in-oil emulsions	> 99.95	–	22,590–48,300	Hu et al. (2015)
PDVB- and PDMAEMA-modified double-layer stainless steel mesh	surfactant-stabilized water-in-oil emulsions	99.32	900–1200	–	Cai et al. (2016)
PPS composite nanofiber membrane	surfactant-stabilized water-in-oil emulsions	99.00	671–1707	–	Kou et al. (2021)
Polymeric sponges	surfactant-free and surfactant-stabilized water-in-oil emulsions	> 99.98	–	up to 155 000	Wang and Chen (2017)
SBS-SSM filter	surfactant-stabilized water-in-oil emulsions	99.90	–	–	Zeng et al. (2017)
Peanut shells powder	surfactant-stabilized water-in-oil emulsions	> 99.50	–	–	Zhao et al. (2020)
PVC/SiO_2 membrane	surfactant-stabilized water-in-oil emulsions	> 95.00	358.6	–	Xu et al. (2021)
ZnO nanoflower@SiC composite ceramic membrane	surfactant-stabilized water-in-hexane emulsion	~ 99	–	~ 1300	Wei et al. (2022)
MnO_2&Carbon sphere composite membrane	surfactant-stabilized water-in-hexane emulsion	> 99.5%	–	3032–15,199	Chen et al. (2022)
PC-aPOSS/CF@PU sponge@ PC-aPOSS/CF	surfactant-free/ surfactant-stabilized water-in-oil emulsions	> 99.93/> 99. 87	–	127,289–248,954/17895–30,157	This work

– Not reported

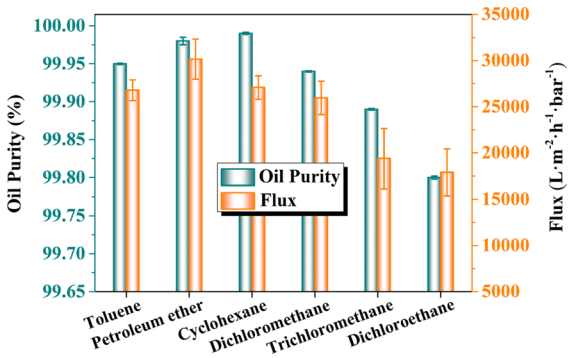

Fig. 9 Oil purities and fluxes for six kinds of surfactant-stabilized water-in-oil emulsions

membrane for separating surfactant-stabilized water-in-oil emulsions.

Figure 10 presents a possible emulsion separation mechanism to give a more comprehensive understanding of the separation process of the composite filter membrane for water-in-oil emulsion. When water-in-oil emulsion approached the composite filter membrane, the emulsified water droplets were captured and coalesced, then were repelled due to the superhydrophobicity of the upper PC-aPOSS/CF. Simultaneously, oil was allowed to pass through the upper PC-aPOSS/CF because of its superoleophilicity. The separation process was referred to

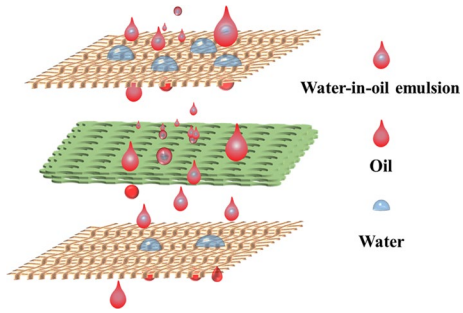

Fig. 10 Separation process of the composite filter membrane for water-in-oil emulsion

the size-sieving filtration and coalescence. The PU sponge in the interlayer has three-dimensional porous structure and amphiphilicity for oil and water. Tiny water droplets could be adsorbed and coalesced with other water droplets to generate larger droplets in the long and interconnected microchannels of the PU sponge. When contacting the bottom superhydrophobic PC-aPOSS/CF, the large water droplets were repelled to achieve complete separation from the emulsion.

Conclusions

This work presents a facile method to fabricate an eco-friendly superhydrophobic/superoleophilic fabric from cardanol/POSS-based polybenzoxazine. The as-prepared superhydrophobic PC-aPOSS/CF had excellent separation performance for various oil/water mixtures, with high oil purity (> 99.86%) and high flux (> 3600 L m^{-2} h^{-1}). Furthermore, the designed composite filter membrane with sandwich-like structure could be used to separate surfactant-free and surfactant-stabilized water-in-oil emulsions upon the application of external pressure. High oil fluxes in the range of 127,289–248,954 and 17,895–30,157 L m^{-2} h^{-1} bar^{-1} were obtained for surfactant-free emulsions and surfactant-stabilized emulsions respectively, with outstanding separation performance (oil purity > 99.86%). More importantly, the superhydrophobic PC-aPOSS/CF exhibited the excellent durability and long-term reusability, which fully meets the requirements for the recovery of oil pollutants. Moreover, the facile and environmentally friendly method will effectively motivate the practical applications of superhydrophobic fabric and expand its application prospects in real life.

Acknowledgments The authors gratefully acknowledge the financial support by the National Natural Science Foundation of China (31700522 and 31901256), and Forestry Science and Technology Innovation and Extension Project of Jiangsu Province (LYKJ[2021]04).

Funding The funding was provided by National Natural Science Foundation of China, 31700522, Qianqian Shang, 31901256,Caiying Bo, Forestry Science and Technology Innovation and Extension Project of Jiangsu Province, LYKJ[2021]04, Lihong Hu.

Declarations

Conflict of interest The authors declare no competing financial interest.

References

Amarnath N, Shukla S, Lochab B (2019) Isomannide-derived chiral rigid fully biobased polybenzoxazines. ACS Sustainable Chem Eng 7(22):18700–18710. https://doi.org/10.1021/acssuschemeng.9b05305

Arumugam H, Ismail AAM, Govindraj L, Muthukaruppan A (2021) Development of bio-based benzoxazines coated melamine foam for oil-water separation. Prog Org Coat 153:106128. https://doi.org/10.1016/j.porgcoat.2020.106128

Bai WB, Lin HM, Chen KH, Xu J, Chen JP, Zhang XM, Zeng RP, Lin JH, Xu YL (2020) Eco-friendly stable cardanol-based benzoxazine modified superhydrophobic cotton fabrics for oil–water separation. Sep Purif Technol 253:117545. https://doi.org/10.1016/j.seppur.2020.117545

Bao Y, Zhang YX, Ma JZ (2020) Reactive amphiphilic hollow SiO_2 Janus nanoparticles for durable superhydrophobic coating. Nanoscale 12:16443–16450. https://doi.org/10.1039/D0NR02571B

Cai YH, Chen DY, Li NJ, Xu QF, Li H, He JH, Lu JM (2016) A facile method to fabricate a double-layer stainless steel mesh for effective separation of water-in-oil emulsions with high flux. J Mater Chem A 4:18815. https://doi.org/10.1039/c6ta08168a

Cao CY, Yi B, Zhang JQ, Hou CS, Wang ZY, Lu G, Huang X, Yao X (2020) Sprayable superhydrophobic coating with high processibility and rapid damage-healing nature. Chem Eng J 392:124834. https://doi.org/10.1016/j.cej.2020.124834

Cassie ABD, Baxter S (1944) Wettability of porous surfaces. Trans Faraday Soc 40:546. https://doi.org/10.1039/tf9444000546

Chen JH, Zhang WP, Wan Z, Li SF, Huang TC, Fei YJ (2019) Oil spills from global tankers: status review and future governance. J Clean Prod 227:20–32. https://doi.org/10.1016/j.jclepro.2019.04.020

Chen XP, Li YM, Yang YS, Zhang D, Guan YH, Bao MT, Wang ZN (2022) A super-hydrophobic and antibiofouling membrane constructed from carbon sphere-welded MnO_2 nanowires for ultra-fast separation of emulsion. J Membrane Sci 653:120514. https://doi.org/10.1016/j.memsci.2022.120514

Devaraju S, Krishnadevi K, Naveena E, Alagar M (2019) Design and development of polybenzoxazine-POSS hybrid materials from renewable starting materials for low k and low surface free energy applications. Mater Res Express 6:104007. https://doi.org/10.1088/2053-1591/ab3ace

Grabowski JH, Powers SP, Roman H, Rouhani S (2017) Potential impacts of the 2010 Deepwater Horizon oil spill on subtidal oysters in the Gulf of Mexico. Mar Ecol Prog Ser 576:163–174. https://doi.org/10.3354/meps12208

Hu L, Gao SJ, Zhu YZ, Zhang F, Jiang L, Jin J (2015) An ultrathin bilayer membrane with asymmetric wettability for pressure responsive oil/water emulsion separation. J Mater Chem A 3:23477. https://doi.org/10.1039/C5TA03975D

Hu DC, Ma WS, Zhang ZL, Ding Y, Wu L (2020) Dual bioinspired design of highly thermally conductive and superhydrophobic nanocellulose composite films. ACS Appl Mater Interfaces 12(9):11115–11125. https://doi.org/10.1021/acsami.0c01425

Klimov VV, Bryuzgin EV, Navrotskiy AV, Novakov IA (2021) Superhydrophobic behavior of coatings based on fluoroalkyl methacrylate copolymers on a textured aluminum surface. Surf Interfaces 25:101255. https://doi.org/10.1016/j.surfin.2021.101255

Kou XH, Han N, Zhang YQ, Tian SW, Li PK, Wang W, Wu C, Li W, Yan XH, Zhang XX (2021) Fabrication of polyphenylene sulfide nanofibrous membrane via sacrificial templated-electrospinning for fast gravity-driven water-in-oil emulsion separation. Sep Purif Technol 275:119124. https://doi.org/10.1016/j.seppur.2021.119124

Li Y, Yu Q, Yin XZ, Xu J, Cai YJ, Han L, Huang H, Zhou YS, Tan YQ, Wang LX, Wang H (2018) Fabrication of superhydrophobic and superoleophilic polybenzoxazine-based cotton fabric for oil–water separation. Cellulose 25:6691–6704. https://doi.org/10.1007/s10570-018-2024-8

Lu RY, Yu YC, Adkhamjon G, Gong WL, Sun XQ, Liu L (2020) Bio-inspired cotton fabric with superhydrophobicity for high-efficiency self-cleaning and oil/water separation. Cellulose 27:7283–7296. https://doi.org/10.1007/s10570-020-03281-9

Lyu Y, Ishida H (2019) Natural-sourced benzoxazine resins, homopolymers, blends and composites: A review of their synthesis, manufacturing and applications. Compos Sci Technol 99:101168. https://doi.org/10.1016/j.progpolymsci.2019.101168

Malakooti S, Qin GQ, Mal C, Soni RS, Taghvaee T, Ren Y, Chen HL, Tsao N, Shiao J, Kulkarni SS, Sotiriou-Leventis C, Leventis N, Lu HB (2019) Low-cost, ambient-dried, superhydrophobic, high strength, thermally insulating, and thermally resilient polybenzoxazine aerogels. ACS Appl Polym Mater 1(9):2322–2333. https://doi.org/10.1021/acsapm.9b00408

Mosayebi E, Azizian S, Noei N (2020) Preparation of robust superhydrophobic sand by chemical vapor deposition of polydimethylsiloxane for oil/water separation. Macromol Mater Eng 305:2000425. https://doi.org/10.1002/mame.202000425

Ning TL, Yang GJ, Zhao W, Liu XK (2017) One-pot solvothermal synthesis of robust ambient-dried polyimide aerogels with morphology-enhanced superhydrophobicity for highly efficient continuous oil/water separation. React Funct Polym 116:17–23. https://doi.org/10.1016/j.reactfunctpolym.2017.04.017

Ogihara H, Katayama T, Saji T (2011) One-step electrophoretic deposition for the preparation of superhydrophobic silica particle/trimethylsiloxysilicate composite coatings. J Colloid Interf Sci 362(2):560–566. https://doi.org/10.1016/j.jcis.2011.06.050

Oliveira LMTM, Saleem J, Bazargan A, Duarte JLDS, Mckay G, Meili L (2021) Sorption as a rapidly response for oil spill accidents: a material and mechanistic approach. J Hazard Mater 407:124842. https://doi.org/10.1016/j.jhazmat.2020.124842

Pal S, Mondal S, Pal P, Das A, Pramanik S, Maity J (2021) Fabrication of durable, fluorine-free superhydrophobic cotton fabric for efficient self-cleaning and heavy/light oil-water separation. Colloid Interfac Sci 44:100469. https://doi.org/10.1016/j.colcom.2021.100469

Park JH, Hu XY, Torfeh M, Okoroanyanwu U, Arbabi A, Watkins JJ (2020) Exceptional electromagnetic shielding efficiency of silver coated carbon fiber fabrics via a roll-to-roll spray coating process. J Mater Chem C 8:11070–11078. https://doi.org/10.1039/D0TC02048F

Prabunathan P, Elumalai P, Kumar GD, Manoj M, Hariharan A, Rathika G, Alaga M (2020) Antiwetting and low-surface-energy behavior of cardanol-based polybenzoxazine-coated cotton fabrics for oil–water separation. J Coat Technol Res 17:1455–1469. https://doi.org/10.1007/s11998-020-00365-w

Qin Y, Li S, Li Y, Pan F, Han L, Chen ZM, Yin XZ, Wang LX, Wang H (2020) Mechanically robust polybenzoxazine/reduced graphene oxide wrapped-cellulose sponge towards highly efficient oil/water separation, and solar-driven for cleaning up crude oil. Compos Sci Technol 197:108254

Renjith PK, Sarathchandran C, Sivanandan Achary V, Chandramohanakumar N, Sekkar V (2021) Micro-cellular polymer foam supported silica aerogel: eco-friendly tool for petroleum oil spill cleanup. J Hazard Mater 415:125548. https://doi.org/10.1016/j.jhazmat.2021.125548

Saji VS (2021) Electrophoretic-deposited superhydrophobic coatings. Chem-Asian J 16(5):474–491. https://doi.org/10.1002/asia.202001425

Sam EK, Ge Y, Liu J, Lv XM (2021) Robust, self-healing, superhydrophobic fabric for efficient oil/water emulsion separation. Colloid Surface A 625:126860. https://doi.org/10.1016/j.colsurfa.2021.126860

Shang QQ, Hu LH, Hu Y, Liu CG, Zhou YH (2018) Fabrication of superhydrophobic fluorinated silica nanoparticles for multifunctional liquid marbles. Appl Phys A 124:25. https://doi.org/10.1007/s00339-017-1446-8

Shang QQ, Chen JQ, Liu CG, Hu Y, Hu LH, Yang XH, Zhou YH (2019) Facile fabrication of environmentally friendly bio-based superhydrophobic surfaces via UV-polymerization for self-cleaning and high efficient oil/water

separation. Prog Org Coat 137:105346. https://doi.org/10.1016/j.porgcoat.2019.105346

Shang QQ, Liu CG, Chen JQ, Yang XH, Hu Y, Hu LH, Zhou YH, Ren XL (2020) Sustainable and robust superhydrophobic cotton fabrics coated with castor oil-based nanocomposites for effective oil-water separation. ACS Sustain Chem Eng 8:7423–7435. https://doi.org/10.1021/acssuschemeng.0c01469

Shang QQ, Cheng JW, Liu CG, Hu LH, Bo CY, Hu Y, Yang XH, Ren XL, Zhou YH, Lei W (2021) Fabrication of sustainable and durable bio-polybenzoxazine based superhydrophobic cotton fabric for efficient oil/water separation. Prog Org Coat 158:106343. https://doi.org/10.1016/j.porgcoat.2021.106343

Si YF, Dong ZC, Jiang L (2018) Bioinspired designs of superhydrophobic and superhydrophilic materials. ACS Cent Sci 4(9):1102–1112. https://doi.org/10.1021/acscentsci.8b00504

Song QQ, Wang HX, Han SQ, Wang J, Zhang B, Zhang YT (2020) Halloysite nanotubes functionalized cotton fabric for oil/water separation. Prog Org Coat 148:105839. https://doi.org/10.1016/j.porgcoat.2020.105839

Wang CF, Chen LT (2017) Preparation of superwetting porous materials for ultrafast separation of water-in-oil emulsions. Langmuir 33:1969–1973. https://doi.org/10.1021/acs.langmuir.6b04344

Wang Z, Zhu HB, Cao N, Du RK, Liu YQ, Zhao GZ (2017) Superhydrophobic surfaces with excellent abrasion resistance based on benzoxazine/mesoporous SiO_2. Mater Lett 186:274–278. https://doi.org/10.1016/j.matlet.2016.10.010

Wang DH, Sun QQ, Hokkanen MJ, Zhang CL, Lin FY, Liu Q, Zhu SP, Zhou TF, Chang Q, He B, Zhou Q, Chen LQ, Wang ZK, Ras RHA, Deng X (2020) Design of robust superhydrophobic surfaces. Nature 582:55–59. https://doi.org/10.1038/s41586-020-2331-8

Wei JJ, Nian P, Wang YX, Wang XJ, Wang YD, Nan Xu, Wei YB (2022) Preparation of superhydrophobic-superoleophilic ZnO nanoflower@SiC composite ceramic membranes for water-in-oil emulsion separation. Sep Purif Technol 292:121002. https://doi.org/10.1016/j.seppur.2022.121002

Xu LH, Liu YD, Yuan XL, Wan J, Wang LM, Pan H, Shen Y (2020) One-pot preparation of robust, ultraviolet-proof superhydrophobic cotton fabrics for self-cleaning and oil/water separation. Cellulose 27:9005–9026. https://doi.org/10.1007/s10570-020-03369-2

Xu HY, Liu HL, Huang Y, Xiao CF (2021) Three-dimensional structure design of tubular polyvinyl chloride hybrid nanofiber membranes for water-in-oil emulsion separation. J Membrane Sci 620:118905. https://doi.org/10.1016/j.memsci.2020.118905

Yao HJ, Lu X, Xin Z, Zhang H, Li X (2019) A durable bio-based polybenzoxazine/SiO_2 modified fabric with superhydrophobicity and superoleophilicity for oil/water separation. Sep Purif Technol 229:115792. https://doi.org/10.1016/j.seppur.2019.115792

Yao HJ, Lu X, Chen SW, Yu CY, He QS, Xin Z (2020) A robust polybenzoxazine/SiO_2 fabric with superhydrophobicity for high-flux oil/water separation. Ind Eng Chem Res 59:7787–7796. https://doi.org/10.1021/acs.iecr.9b06003

Zeng XJ, Qian L, Yuan XX, Zhou CL, Li ZW, Cheng J, Xu SP, Wang SF, Pi PH, Wen XF (2017) Inspired by stenocara beetles: from water collection to high-efficiency water-in-oil emulsion separation. ACS Nano 11:760–769. https://doi.org/10.1021/acsnano.6b07182

Zhang H, Hou CP, Song LX, Ma Y, Ali Z, Gu JW, Zhang BL, Zhang HP, Zhang QY (2018) A stable 3D sol-gel network with dangling fluoroalkyl chains and rapid self-healing ability as a long-lived superhydrophobic fabric coating. Chem Eng J 334:598–610. https://doi.org/10.1016/j.cej.2017.10.036

Zhang N, Qi YF, Zhang YN, Luo JL, Cui P, Jiang W (2020a) A review on oil/water mixture separation material. Ind Eng Chem Res 59:14546–14568. https://doi.org/10.1021/acs.iecr.0c02524

Zhang S, Zong JP, Ran QC, Gu Y (2020b) Facile preparation of lightweight and robust polybenzoxazine foams. Ind Eng Chem Res 59(16):7575–7583. https://doi.org/10.1021/acs.iecr.0c00313

Zhang WL, Wang DH, Sun ZN, Song JN, Deng X (2021) Robust superhydrophobicity: mechanisms and strategies. Chem Soc Rev 50:4031–4061. https://doi.org/10.1039/D0CS00751J

Zhao BW, Ren LY, Du YB, Wang JY (2020) Eco-friendly separation layers based on waste peanut shell for gravity-driven water-in-oil emulsion separation. J Clean Prod 255:120184. https://doi.org/10.1016/j.jclepro.2020.120184

Zheng ZR, Gu ZY, Huo RT, Ye YH (2009) Superhydrophobicity of polyvinylidene fluoride membrane fabricated by chemical vapor deposition from solution. Appl Surf Sci 255:7263–7267. https://doi.org/10.1016/j.apsusc.2009.03.084

Zhu SW, Yang XJ, Li TH, Li F, Cao W (2017) Phase and morphology controllable synthesis of superhydrophobic Sb_2O_3 via a solvothermal method. J Alloy Compd 721:149–156. https://doi.org/10.1016/j.jallcom.2017.05.327